

$J=0$ curve between convex and saddle regions; (b) An inner square corresponding to the $J=0$ curve between concave and saddle regions. Likewise the TA_2 mode produces the narrow diagonal ramps. Within the angular resolution of our bolometer (1°), all of these calculated details are confirmed in the photographs. Both the pattern and scale of the images agree well with the calculated infinities in the enhancement factor A with use of the known elastic constants of Ge.

We believe that this type of experiment and analysis provides useful insights into the phenomenon of phonon focusing. The detailed ballistic phonon patterns are a sensitive experimental probe of the fundamental constant energy surfaces for elastic waves. We further expect that this scanning method may prove useful as a probe of phonon interactions with crystalline defects and photoexcited phases in semiconductors.

We are indebted to A. C. Anderson for his encouragement and essential help in fabricating the superconducting detector. M. A. Tamor interfaced the minicomputer system which proved essential to this work. We thank M. Greenstein for his frequent advice and assistance. This work was supported by the National Science Foundation under the Materials Research Laboratory Grant No. DMR-77-23999, with equipment support by National Science Foundation Grant No. DMR-77-11672 and a Cottrell Research Grant.

¹See, for example, M. J. P. Musgrave, *Crystal Acoustics* (Holden-Day, San Francisco, 1970); F. I. Federov, *Theory of Elastic Waves in Crystals* (Plenum, New

York, 1968).

²B. Taylor, H. J. Maris, and C. Elbaum, *Phys. Rev. Lett.* **23**, 415 (1969).

³E. B. Christoffel, *Ann. Mat. Pura Appl.* **8**, 193 (1977).

⁴H. J. McSkimin and P. Andreatch, *J. Appl. Phys.* **34**, 651 (1963).

⁵B. Taylor, H. J. Maris, and C. Elbaum, *Phys. Rev. B* **3**, 1462 (1971).

⁶M. Pomerantz and R. J. von Gutfeld, in *Proceedings of the International Conference on the Physics of Semiconductors, Leningrad, 1967*, edited by S. M. Ryvkin and Yu. V. Shmartser (Nauka, Leningrad, 1968), Vol. 2, p. 670.

⁷J. C. Hensel and R. C. Dynes, *Physics of Semiconductors—1978* The Institute of Physics Conference Proceedings No. 43, edited by B. L. H. Wilson (The Institute of Physics, Bristol and London, 1978), p. 371.

⁸R. J. von Gutfeld and A. H. Nethercot, Jr., *Phys. Rev. Lett.* **12**, 641 (1964).

⁹For a description of the method, see R. J. von Gutfeld, *Physical Acoustics* (Academic, New York, 1968), Vol. 5, p. 223.

¹⁰A $10 \times 10 \times 10$ -mm³ crystal with $N_D - N_A \approx 10^{12}$ cm⁻³, grown by E. E. Haller and W. L. Hansen of Lawrence Berkeley Laboratory.

¹¹A constantan or aluminum film ~ 2000 Å thick was vacuum deposited on one face. Similar focusing was observed, however, for a polished surface, where phonons from photoproduced carrier thermalization generated the heat pulse.

¹²This image took 10 min to accumulate with signal averaging. A complete image could be obtained in less than a minute, with some sacrifice of signal-to-noise ratio.

¹³F. Rösch and O. Weis, *Z. Phys. B* **25**, 101, 115 (1976).

¹⁴H. J. Maris, *J. Acoust. Soc. Amer.* **50**, 812 (1971).

¹⁵A. G. Every, *Phys. Rev. Lett.* **42**, 1065 (1979).

Zone-Boundary-Phonon Raman Scattering in VI_2 due to Modulation of Exchange Interaction

G. Güntherodt, W. Bauhofer, and G. Benedek^(a)

Max-Planck-Institut für Festkörperforschung, Stuttgart, Federal Republic of Germany

(Received 4 June 1979)

Three new Raman lines appearing below the antiferromagnetic ordering temperature of VI_2 are attributed to zone-boundary-phonon Raman scattering induced by the elastic ("Bragg") magnetic scattering from the spin superstructure. The spin-dependent electron-phonon coupling is explained in terms of a modulation of the exchange interactions by selected zone-boundary phonons.

Phonon-induced modulation of exchange interactions below the ordering temperature of magnetic crystals may provide an additional spin-

dependent electron-phonon (EP) coupling mechanism in Raman scattering (RS). The previous work of Steigmeier and Harbeck¹ on RS in Cd-Cr

spinel has stimulated theoretical work in this direction. The strongly temperature-dependent RS, following a spin correlation function below the Curie temperature T_C , had been attributed to a modulation of the superexchange interaction by phonons.² Recent experiments, however, revealed that this observation is rather due to resonant RS, where interband transitions undergoing exchange splittings below T_C are involved.^{3,4}

In this work we present the first evidence of spin-dependent phonon RS in a transition-metal compound induced by a modulation of the exchange interaction through selected phonon modes. In VI_2 we have found with the onset of antiferromagnetic long-range order ($T_N=15\text{ K}$)⁵ an abrupt appearance of three new Raman lines. They are attributed to inelastic scattering from zone-boundary phonons induced by the elastic ("Bragg") magnetic scattering from the spin superstructure.

The VI_2 samples used in our experiments were of the red type having the CdI_2 structure with

D_{3d}^3 space-group symmetry.⁶ The room-temperature Raman spectrum of VI_2 in Fig. 1 shows the two Raman-active E_g and A_{1g} modes. The weak structure appearing above 200 cm^{-1} is attributed to second-order RS. Below T_N we observe three new Raman lines at 66 , 195 , and 220 cm^{-1} . Some possible explanations for these new lines, appearing in both scattering geometries, such as (a) one-magnon RS, (b) phonon-magnon excitations, (c) two-magnon RS, or (d) concurrent magnetic and structural phase transition, can be ruled out by the following arguments: For cases (a) and (b), the low-temperature spectra (14 K down to 2 K) did not show any change in external magnetic fields up to 12 T perpendicular or parallel to the c axis; moreover, this RS should appear dominantly in the $z(xy)\bar{z}$ geometry.⁷ For case (c), because of the large antiferromagnetic short-range-order region above T_N ,⁸ the two-magnon RS should persist at temperatures far above T_N ,⁹ contrary to our observations. Indeed, the integrated intensities of the new lines depend on temperature (inset of Fig. 1) as qualitatively predicted by Suzuki and Kamimura² for phonon RS induced by exchange-energy modulation ($R=K=0$ in Ref. 2). As for case (d), low-temperature neutron-scattering experiments⁸ give no evidence for a structural change at T_N .

The antiferromagnetic structure of VI_2 below T_N has been reported recently.⁸ The result is shown in Fig. 2(a) for the x - y plane, into which we have projected the spins lying actually in the y - z plane under 60° with respect to the y axis. The eight spins belonging to the magnetic unit cell are shown in Fig. 2(b). Since the magnetic

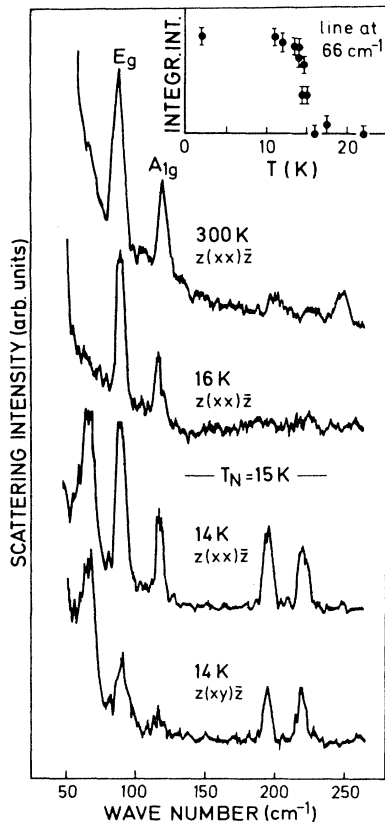


FIG. 1. Raman spectra of VI_2 (exciting wavelength is 4765 \AA) as a function of temperature. The inset shows the temperature dependence of the integrated intensity of the 66-cm^{-1} line in $z(xx)\bar{z}$ geometry. Similar behavior is found for the lines at 195 and 220 cm^{-1} .

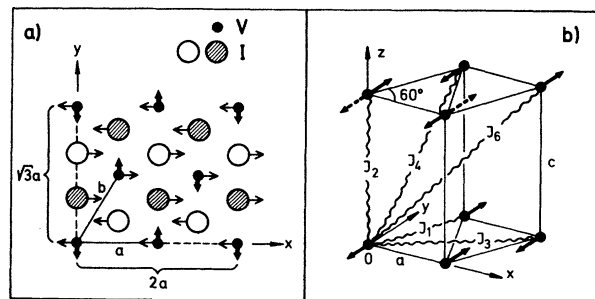


FIG. 2. Spin structure (thick arrows) of VI_2 (a) within the layer and (b) for $\frac{1}{8}$ the volume of the magnetic cell according to Ref. 8 (see text). a , b , and c are the basis vectors of the crystallographic cell; $2a$, $3\frac{1}{2}a$, and $2c$ are the dimensions of the magnetic cell. The displacement field of A_u modes is also shown (thin arrows).

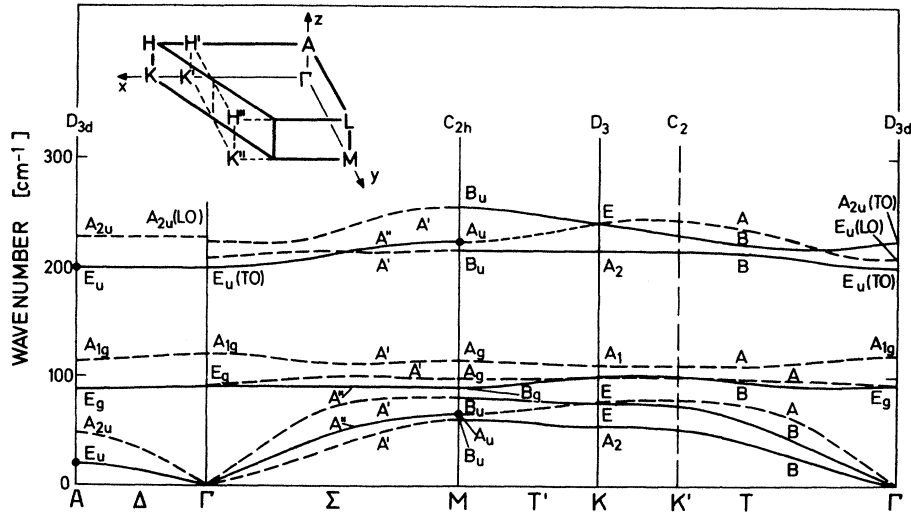


FIG. 3. Calculated phonon dispersion curves of VI_2 at 300 K (Ref. 11). The inset shows $\frac{1}{8}$ of the crystallographic Brillouin zone (solid lines).

unit cell includes eight molecules we obtain 72 phonon branches. In the antiferromagnetic phase the points $K' = (\pi/a, 0, 0)$, $M = (0, 2\pi/\sqrt{3}a, 0)$, and $A = (0, 0, \pi/c)$ (inset of Fig. 3) represent the new reciprocal-lattice basis vectors and, together with the points H' , L , K'' , and H'' , are equivalent to Γ . Hence, new $q=0$ optical modes appear from the corresponding folding of the phonon branches. Since the point group of the magnetic cell is C_{2h} (C_2 axis along $(1, -\sqrt{3}, 0)$), the 36 Raman-active modes transform like either A_g or B_g . But only the modes providing a modulation

of either the spin-orbit coupling constant λ or the exchange interaction constant J would activate, to lowest order in the EP interaction, spin-dependent phonon RS. The modulation of λ can occur via the even component of the ligand displacements around each V ion. However, the individual contributions from the eight molecules of the magnetic unit cell cancel each other for all Raman-active modes, except for the original ones (E_g, A_{1g}).

As concerns the phonon modulation of the exchange energy, we write the spin-dependent EP interaction in the following form:

$$H_{EP} = (2N)^{-1} \sum_{\vec{q}\lambda} Q_{\vec{q}\lambda}(t) \sum_l \exp^{i\vec{q}\cdot\vec{r}_l} \sum_{i \neq j} \sum_{\kappa} [\sum_{\kappa} \vec{w}(\kappa|\vec{q}\lambda) \cdot (\partial J_{ij}/\partial \vec{r}_{l\kappa})] \vec{S}_i \cdot \vec{S}_j, \quad (1)$$

where $Q_{\vec{q}\lambda}(t)$ and $\vec{w}(\kappa|\vec{q}\lambda)$ are normal-coordinate operator and the polarization vector, respectively, for wave vector \vec{q} and branch index λ ; $\vec{r}_{l\kappa} = \vec{r}_l + \vec{r}_{\kappa}$ is the position of the κ th atom in the l th crystallographic cell ($l=1, 2, \dots, N$). J_{ij} is the exchange constant between spins i and j in the magnetic cell; and $\partial J_{ij}/\partial \vec{r}_{l\kappa} \equiv \hat{i} \partial J_{ij}/\partial x_{l\kappa} + \hat{j} \partial J_{ij}/\partial y_{l\kappa} + \hat{k} \partial J_{ij}/\partial z_{l\kappa}$. How this interaction contributes to the RS cross section has been investigated theoretically for different magnetic regimes.^{2,10} Here we want to show the strict link between selected phonons and spin structure. The summation $\sum_{i \neq j}$ in Eq. (1) yields a scalar quantity having the same periodicity as the magnetic lattice. Hence

$$H_{EP} = \sum_{\vec{g}} \sum_{\vec{q}\lambda} Q_{\vec{q}\lambda}(t) \epsilon_{-\vec{g}}(\vec{q}\lambda) \delta(\vec{q} - \vec{g}), \quad (2)$$

where \vec{g} are reciprocal vectors of the magnetic lattice and $\epsilon_{-\vec{g}}(\vec{q}\lambda)$ contains the information on the spin-phonon coupling. This coupling activates RS from phonons with $\vec{q} = \vec{g}$, provided that $\epsilon_{-\vec{g}} \neq 0$. The momentum conservation is assured by the elastic ("Bragg") scattering in the spin system ($-\vec{g}$). The coefficients $\epsilon_{-\vec{g}}$ are determined by inspection of the spin arrangement.

The spin structure of Fig. 2(a) yields one Fourier component for $\vec{g} = M$. Furthermore, the scalar product in Eq. (1) selects only A_u modes whose eigenvectors $\vec{w}^+(\vec{q}, A_u)$ are polarized along the x axis. The schematic displacement pattern of the acoustic A_u mode at point M has been indicated by thin arrows in Fig. 2(a). For the optic A_u mode the same pattern applies for the V ions,

whereas the I ions are at rest. Looking at the calculated phonon dispersion curves of VI_2 in Fig. 3,¹¹ we see that there are two A_u modes at the M point whose frequencies (65 and 223 cm^{-1}) are in good agreement with two of the three new Raman frequencies in Fig. 1. We point out that the superexchange interactions are modulated also by the iodine displacements, a fact which explains the strong contribution of the acoustic A_u mode to the observed scattering.

The above analysis, based on the spin structure reported by Kuindersma *et al.*,⁸ does not explain the peak observed at 195 cm^{-1} in Fig. 1. This peak presumably arises from the combination $A_{1g}(\Gamma) + A_u(M)$. There is, however, another intriguing coincidence of this peak with the E_u optical mode at point A . The activation of the latter mode in RS depends on the stacking of spins along the c axis. Since there is still some controversy about the actual spin orientations,¹² it is worth noting the existence of other spin arrangements within the same magnetic cell as of Ref. 8 which explain all three new Raman lines. This alternative structure, resulting from a reversal of two spins [Fig. 2(b), broken arrows], contains two Fourier components with $\vec{g} = A$ and $\vec{g} = L$ because of interlayer and intralayer exchange interactions, respectively. Again, the phonons involved are polarized along x and are $E_{u,x}$ at point A (20 and 199 cm^{-1}) and A_u at point L (62 and 224 cm^{-1}) in good agreement with the experimental frequencies. The predicted mode at 20 cm^{-1} , however, could not be resolved (see Fig. 1) because of the strong elastic scattering.

The insensitivity on scattering geometry of the three new Raman lines for $T < T_N$ (see Fig. 1) is a consequence of the fact that the point groups of M and L (C_{2h}) and of A (D_{3d}) contain a horizontal C_2 axis, forming an angle $\alpha = 60^\circ$ with the C_2 axis of the magnetic unit cell. Therefore, A_u as well as E_u modes are folded into a mixture $A_g \times \cos\alpha + B_g \sin\alpha$. For an order-of-magnitude estimate of the coupling strength of our proposed mechanism we approximate the derivative $\partial J / \partial r \sim -J/\rho$, where $\rho = 0.17 \text{ \AA}$ is the Born-Mayer repulsive parameter¹¹ and consider $|J| = 7.8 \text{ K}$ for the intralayer interactions.⁸ Taking into account in first approximation only the six first-neighbor spins, we obtain for the optical A_u (L) mode an EP coupling per magnetic cell of the order of 100 cm^{-1} . This represents just a lower limit of the ground-state EP interaction. A larger contribution is expected from the exchange interaction in the virtual excited state. Therefore this

should be comparable with the orbital EP interaction, which, for a crystal-field transition, is of the order of $|\vec{w}\partial(10Dq)/\partial r_0| \sim 50|\vec{w}/r_0|Dq \sim 50 \text{ cm}^{-1}$, where r_0 is the nearest-neighbor distance and $Dq = 787 \text{ cm}^{-1}$.⁵

Actually, $q \neq 0$ phonon RS induced by magnetic "Bragg" scattering has been observed in the europium chalcogenides,¹³ where the spin-phonon excitation is due to the spin-orbit coupling in the excited intermediate state.¹⁴ Such a second-order RS mechanism is negligible in our present case since the spin-orbit coupling is one order of magnitude smaller. In view of the extensive work carried out on RS of transition-metal compounds,¹⁵ why has the above first-order RS process not been observed previously? The RS mechanism found in VI_2 is apparently rare, despite its simplicity. It could provide a useful tool, complementary to neutron scattering techniques, for unraveling relatively complex spin structures with $\vec{g} \neq \Gamma$.

We thank E. Anastassakis and G. Abstreiter for cooperation in the experiments, A. Frey for the lattice-dynamical calculations, and L. Reatto, H. Bilz, and M. Cardona for fruitful discussions.

(a)Permanent address: Gruppo Nazionale di Struttura della Materia del Consiglio Nazionale delle Ricerche, Istituto di Fisica dell'Università, Milano, Italy.

¹E. F. Steigmeier and G. Harbeke, Phys. Condens. Matter **12**, 1 (1970).

²N. Suzuki and H. Kamimura, J. Phys. Soc. Jpn. **35**, 985 (1973); N. Suzuki, J. Phys. Soc. Jpn. **40**, 1233 (1976).

³N. Koshizuka, Y. Yokoyama, and T. Tsushima, Solid State Commun. **18**, 1333 (1976).

⁴M. Iliev, G. Güntherodt, and H. Pink, Solid State Commun. **27**, 863 (1978).

⁵W. van Erk and C. Haas, Phys. Status Solidi (b) **71**, 537 (1975).

⁶G. Lamprecht and E. Schönherr, to be published.

⁷P. A. Fleury and R. Loudon, Phys. Rev. **166**, 514 (1968).

⁸S. R. Kuindersma, C. Haas, J. P. Sanchez, and R. Al, Solid State Commun. **30**, 403 (1979).

⁹P. A. Fleury, Phys. Rev. **180**, 591 (1969).

¹⁰O. Sakai and M. Tachiki, J. Phys. Chem. Solids **39**, 269 (1978).

¹¹A. Frey and G. Benedek, to be published.

¹²K. R. A. Ziebeck, private communication.

¹³R. P. Silverstein, L. E. Schmutz, V. I. Tekippe, M. S. Dresselhaus, and R. L. Aggarwal, Solid State Commun. **18**, 1173 (1976).

¹⁴R. Merlin, R. Zeyher, and G. Güntherodt, Phys. Rev. Lett. **39**, 1215 (1977).

¹⁵J. W. Johnstone, D. J. Lockwood, and G. Mischler, J. Phys. C **11**, 2147 (1978), and references therein.